Modified scaba 6SRGT impellers for process intensification: Cavern size and energy saving when stirring viscoplastic fluids

H Ameur, Christophe Vial

▶ **To cite this version:**

H Ameur, Christophe Vial. Modified scaba 6SRGT impellers for process intensification: Cavern size and energy saving when stirring viscoplastic fluids. Chemical Engineering and Processing: Process Intensification, 2020, 148, pp.107795. 10.1016/j.cep.2019.107795 . hal-03086119

HAL Id: hal-03086119
https://uca.hal.science/hal-03086119

Submitted on 22 Dec 2020

HAL is a multi-disciplinary open access archive for the deposit and dissemination of scientific research documents, whether they are published or not. The documents may come from teaching and research institutions in France or abroad, or from public or private research centers.

L'archive ouverte pluridisciplinaire **HAL**, est destinée au dépôt et à la diffusion de documents scientifiques de niveau recherche, publiés ou non, émanant des établissements d'enseignement et de recherche français ou étrangers, des laboratoires publics ou privés.

Distributed under a Creative Commons Attribution 4.0 International License

Mixing of Hershel-Bulkley fluids by Scaba 6SRGT impellers in cylindrical tanks: Effect of cuts in the blades

Houari Ameur[1,*], Christophe Vial[2,3]

[1]Département de Technologie, Centre Universitaire de Naama (Ctr Univ Naama), BP 66, 45000, Algeria

[2]Université Clermont Auvergne, Université Blaise Pascal, Institut Pascal, BP 10448, F-63000 Clermont-Ferrand, France

[3]CNRS, UMR 6602, IP, F-63178 Aubière, France

Correspondance. E-mail: houari_ameur@yahoo.fr; Tel.: +213770343722

Abstract: Mixing of a shear-thinning fluid with yield stress using Scaba 6SRGT impellers in a cylindrical unbaffled vessel is studied. Cuts are introduced in each blade of the impeller in order to reduce power requirements. The effects of the cut-height (five geometrical configurations: h_2/D = 0, 0.015, 0.04, 0.065 and 0.09, respectively), cut-length (four shapes: l/D = 0, 0.06, 0.12 and 0.18, respectively) , and of the number of cuts (n_b = 1, 2, 3, 4, and 5) on the hydrodynamics and power consumption are explored. From the simulations, it can be inferred that the introduction of cuts is an interesting technique to obtain an energy-saving impeller. The suggested designs, compared to the classical Scaba 6SRGT impeller, display a reduction in power number by about 20%, 19.9% and 66.6% when the cut-height, cut-length and number of cuts are changed from h_2/D = 0 to 0.09, l/D = 0 to 0.18 and n_b = 1 to 5, respectively. However, the increased surface area of cuts in the blades is accompanied by a reduction in the size of radial jet of fluid, resulting thus in a weakened axial flow and a decrease in cavern size. As a result, the best trade-off between the reduced power consumption and enlarged cavern size correspond to the case n_b = 3, l/D = 0.12. The reduction in power number for this case is estimated to be as about 15%.

Keywords: Mixing; Shear thinning fluids; Curved bladed impeller; cut in blade.

1. Introduction

Mechanical agitation of fluids in cylindrical tanks is a fundamental operation in to achieve a wide variety of tasks, such as gas dispersion into liquid to form foams or for mass transfer, powder dispersion or solid blending, dispersion of immiscible liquids for emulsification, preparation of ingredients, etc. Various shapes of impellers have been developed for mixing complex non-Newtonian fluids encountered in different industries and the control of complex fluid flows is highly required to optimize the processes. Shear-thinning fluids with yield stress present the most common class of this kind of fluids, and they are characterized by a great increase in viscosity when the shear stresses are less than the yield stress. For this reason, many challenging problems are encountered during the mixing process such as higher mixing time, low heat transfer, fouling and buildup on the walls, formation of gel, formation of well-mixed regions near the stirrer (the so-called caverns) with stagnant/dead regions elsewhere (Rudolph et al., 2009; Bao et al., 2011). The product quality is highly affected by the formation of these glitches; so, a sophisticated designed impeller should be selected to overcome, i.e. eliminate or at least minimize, the above-mentioned issues.

Radial flow is the main source of mising intensification in stirred tank reactors. Ameur (2016a) and Zhao et al. (2011) reported that trailing vortices generated behind flat-bladed impellers are the main source of energy dissipation. In aerated agitation, these vortices (filled with gas) are also responsible for the formation of cavities, which yields a reduction in mass transfer and unstabilities in power consumption (Zheng et al., 2017). This issue has been overcome by the development of impellers exhibiting semi-circular tube blades (CD), and the evolution of the flow field between the CD-6 impeller and Rushton turbine (RT) has been deeply analyzed by Devi and Kumar (2013). Since then, engineers and researchers have been more and more interested in the development and the use of impellers with deeper concaved blades (Pakzad et al., 2008a, 2008b; Ghotli et al., 2013, 2016; Cortada-Garcia et al., 2017; Malik and Pakzad, 2018). Impellers with different shapes of blades have been compared by Zhao et al. (2011): namely, the flat (Rushton turbine), half-elliptical, concave, and parabolic shapes. These authors found an increase in the residence time of vortex at the impeller tip with the rise of blade curvature, which yields also stronger and smaller vortices in this region. The space between the lower and upper vortices presented the location of high turbulent kinetic energy. Recently, Zheng et al. (2018) also designed a new fan-shaped impeller assembled with annular-sector-shaped concave blades. With this new design, they found a reduction in power number by 26% compared to that of the Bakker turbine. For shear-thinning fluids with yield

stress, research have been focused on the Scaba impellers under different operating and geometrical conditions, including the coaxial, multistaged, and the multiple eccentric configurations (Pakzad et al. 2013a, 2013b, 2013c; Kazemzadeh et al., 2016a, 2016b, 2017; Ameur, 2016b, Ameur and Ghenaim, 2018).

Thus, the main purpose of this paper is to propose an original way to save mechanical power when curved-bladed impellers (Scaba 6SRGT) are used for mixing shear-thinning fluids with yield stres: this consists in introducing cuts in the impeller blades, the geometry of which must be optimized. As a result, the effects of the cut size (including the cut-length, cut-height and the numbers of cut) on the flow patterns, caverns size and power consumption have been investigated in detail in the next sections.

2. Experimental setup

The mechanically stirred tank under study is a flat-bottomed cylindrical unbaffled vessel equipped with a Scaba 6SRGT impeller (Fig. 1). The impeller has six curved blades mounted on on a disc with a thickness t/D = 0.02, where D is the vessel diameter (D= 0.4 m). The impeller shaft has a diameter d_s/D = 0.05. The shaft is inserted at the central position of impeller and the off-bottom clearance is c/D = 0.33. The liquid level is kept equal to the vessel height H, where H/D = 1. All other details are summarized in Table 1.

Cuts have been introduced in the impeller blade in order to reduce power supply. For this purpose, fourteen geometrical configuration were investigated to assess the effects of the geometry of the cuts: namely, five geometries with changes in the height of cut (h_2/D = 0, 0.015, 0.04, 0.065 and 0.09, respectively), four geometries with changes in the length of cut (l/D = 0, 0.06, 0.12 and 0.18, respectively) and five geometries with changes in the number of cuts (n_b = 1, 2, 3, 4 and 5).

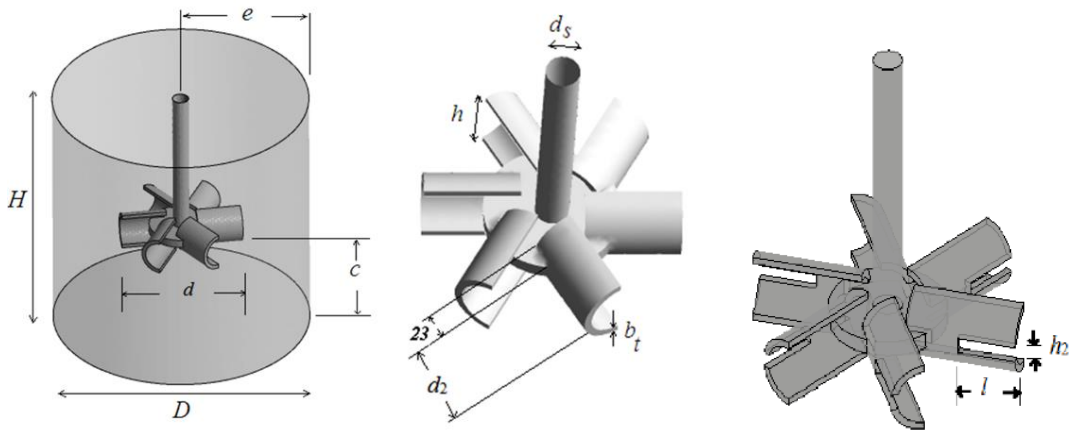

(a) (b) (c)

Figure 1. Geometry of the stirred tank (a); design of the classical Scaba 6SRGT impeller (b); and design of the modified Scaba 6SRGT impeller (c)

Table 1. Mixing system geometrical features

D [mm]	*H/D*	*d/D*	*c/D*	*h/D*	d_s/D	b_t/D
400	1	0.47	0.33	0.1	0.05	0.015

3. Mathematical equations

A xanthan gum solution was utilized as the working fluid in this paper. Based on the experimental measurements reported by Saeed et al. (2007) and Pakzad et al. (2008b), the rheological propeties of this fluid are: concentration 10.5%, consistency index $K = 3$ [Pa s^n], power law index $n = 0.11$, yield stress $\tau_y = 1.79$ [Pa] and density $\rho = 991.8$ [kg/m^3]. The behavior of this fluid is shear-thinning with yield stress and it can be modeled using the Herschel-Bulkley model (Macosko, 1994):

$$\tau = \tau_y + K\dot{\gamma}^n \tag{1}$$

In the flow regime, the average shear rate can be related to the stirrer rotational speed by the Metzner and Otto's approach (Metzner and Otto, 1957):

$$\dot{\gamma}_{avg} = K_s N \tag{2}$$

Thus, the apparent viscosity of the fluid, η, can be evaluated from the average shear rate, as follows:

$$\eta = \frac{\tau}{\dot{\gamma}_{avg}} = \frac{\tau}{k_s N} = \frac{\tau_y + K\left(K_s N\right)^n}{K_s N} \tag{3}$$

For this class of fluids, the Reynolds number is defined as:

$$Re_y = \frac{K_s N^2 d^2 \rho}{\tau_y + K\left(K_s N\right)^n} \tag{4}$$

The pumping flow rate (Q_p), also called the pumping capacity or the delivery rate of the impeller, is the amount of liquid that leaves the impeller blade per unit of time. It is calculated as:

$$Q_p = \pi d \int_0^h V_r \, dz \tag{5}$$

where V_r is the radial velocity at the blade tip and Z is the position of a point at the height of the blade.

The power consumption (P) can be deduced by numerical integration on the tank volume of the local power transmitted by the impeller to the fluid.

$$P = \eta \int_{vessel\ volume} Q_v \, dv \tag{6}$$

The element dv can be written as:

$$dv = r \, dr \, d\theta \, dz \tag{7}$$

$$Q_v = \left(2\tau_{rr}^2 + 2\tau_{\theta\theta}^2 + 2\tau_{zz}^2 + \tau_{rz}^2 + \tau_{r\theta}^2 + \tau_{z\theta}^2\right)/\eta^2 \tag{8}$$

$$\tau_{rr} = -\eta \, 2\partial v_r / \partial r \tag{9}$$

$$\tau_{r\theta} = -\eta\left[r\,\partial\left(v_\theta / r\right)/\partial r + \left(1/r\right)\partial v_r / \partial\theta\right] \tag{10}$$

$$\tau_{rz} = -\eta\left[\,\partial v_r / \partial z + \partial v_z / \partial r\right] \tag{11}$$

But it can also be deduced by numerical estimation of the torque estimated on the surface of the

impeller. The power number and flow number are calculated respectively as:

$$N_P = \frac{P}{\rho N^3 d^5} \tag{12}$$

$$N_Q = \frac{Q_p}{N d^3} \tag{13}$$

In the dimensionless form, we can define the dimensionless radial and axial coordinates, respectively, as:

$$Z^* = Z/D,\ R^* = 2R/D \tag{14}$$

The dimensionless velocity is also expressed as:

$$V^* = V/\pi Nd \tag{15}$$

and the axial, radial and tangential velocity components can be adimensionalized using the same equation.

4. Numerical methods

The study was conducted using CFD (Computational Fluid dynamics) with the help of the software commercial software package CFX, which is based on the finite volume method and solves the Navier-Stokes equations. Geometry and mesh of the computation domain were created using computer-aided design and meshing software ICEM CFD. The continuity and momentum equations written in a cylindrical and rotating frame of references were solved. Due to the absence of baffles, the Rotating Reference Frame (RRF) approach was used, i.e. the mixer is kept stationary and the vessel is given an angular velocity equal and opposite to the velocity of the rotating frame. The efficiency of this technique was proved by many researchers (Beloudane et al., 2018; Foukrach et al., 2019). Coriolis and centrifugal accelerations are added to the governing equations because of the choice of a rotating frame. Thus, the flow is supposed to be steady, laminar, and isothermal. The pressure-velocity coupling is performed using the SIMPLEC (Semi-Implicit Method for Pressure- Linked Equations-Consistent) algorithm.

Tetrahedral grid elements were used to discretize the computational domain and increased mesh density was created near the impeller and vessel walls in order to determine the details of the fluid boundary layer. After mesh tests, the selected mesh which did not give changes in power consumption higher than 2.5%, had about 0.8 million cells. With a machine (INTEL® i7 processor

with 8 Gb RAM) and for a residual target 10^{-7}, the convergence was achieved after about 700−800 iterations, which corresponds to about 4−5 hrs. CPU time.

5. Validation of simulations with experimental data

The validation of some of the predicted results with the available experimental data is discussed in this section. To validate the simulations, we referred to the experimental work performed by Pakzad et al. (2008b) and we simulated the same geometry as in this paper. The numerical estimations of the flow number vs. impeller rotational speed are displayed in Fig. 2 for the 0.5% xanthan gum solution. The relevance of the physical model, including the boundary conditions, and the accuracy of the numerical parameters of the solver is confirmed by the comparison between numerical and experimental results in Fig. 2 which reveals a very satisfactory agreement.

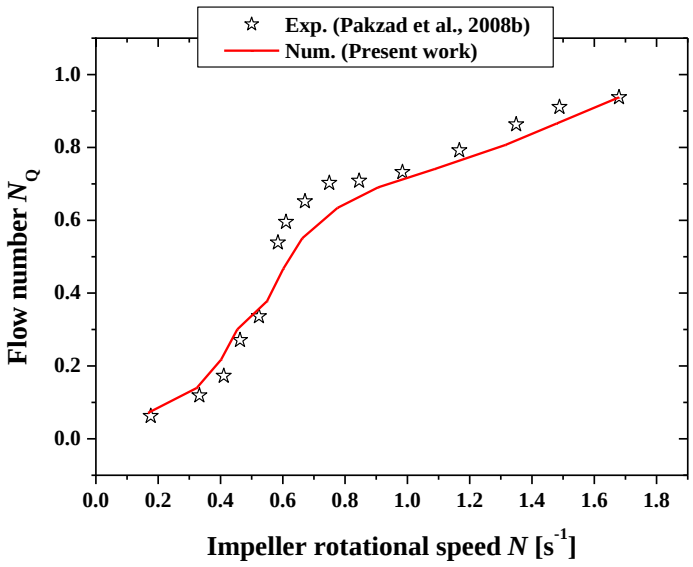

Figure 2. Flow number vs. impeller rotational speed for the 0.5% xanthan gum

6. Results and discussion

6.1. Effect of the height of cut in blades (h_2)

In the first part of our investigation, we explored the effect of the height (h_2) of cut in blade son the flow patterns and power consumption. For this purpose, the five geometrical

configurations described in section 2 with h_2/D between 0 (i.e. a plain blade without cut) and 0.09 have been investigated.

The tangential velocity (V_θ^*) is presented in Fig. 3 along the dimensionless radial coordinate (R^*) at the angular position θ = 0° when vertical coordinate is Z^* = 0.4 (which corresponds to the line passing through the mid-height of the blade. As observed in this figure, the tangential velocity increases first gradually from the impeller shaft and along the blade length until reaching its maximum value at the blade tip. Then, it decreases continuously until becoming negligible at the tank wall. This figure also reveals that and the tangential flow is maximized by the conventional impeller design (h_2/D = 0), as expected, and that it decreases with increasing the height of cut in blade. It must, however, be pointed out that when h_2/D = 0.015, the predicted velocity values are very close to those calculated for the conventional impeller; this highlights that if the height remains very small, the flow still follows the blade even in the region where it has been cut, which is probably reinforced by the shear-thinning character of the fluid.

Similarly, the evolution of the radial velocity along the vessel height is plotted in Fig. 4 for the angular position θ = 0° and a radial position close to the blade tip (R^* = 0.4). As expected, the velocity peak of the radial impinging jet 6SRGT impeller is maximized for the conventional mixing device, and decreases with increased height of cut. It is halved when h_2/D > 0.065.

For further knowledge on the hydrodynamics induced by both the classical and modified Scaba impellers, the streamlines are plotted in Fig. 5 under a two-dimensional view in a vertical plane passing through the blade. Whatever the height of cut, the flow ejected from the blade is directed horizontally towards the vessel wall and it is divided into two streams: one going up to the free surface of liquid, and the other flowing down to the flat bottom of the vessel. Consequently, two recirculation loops are formed, respectively above and below the impeller. it must be pointed out that the cuts do not alter this flow pattern, but the interesting phenomenon illustrated by the slices of this figure is the evolution of the size of eddies yielded by the turbine: The smaller h_2/D, the wider eddies. This is mainly due to the reduction of radial flow with the raise of h_2/D, as claimed above. Consequently, the limited axial circulation of the fluid is another consequence of the increased height of cut in blade, since the area swept by the turbine is more and more reduced, resulting thus in a reduced size of the cavern (well-stirred region), as observed in Fig. 6. But as observed in Fig. 3 and Fig. 4, this effect is weak when h/D< 0.015.

What about the other factors determining of the performance of a stirred system? Here, we can focus first on the change in the power requirements with cut height. Power number (N_P) data is summarized in Fig. 7 for the five geometrical configurations; the values are N_P = 9.5,

9.1, 8.5, 7.9 and 7.6 for h_2/D = 0, 0.015, 0.04, 0.065 and 0.09, respectively. The analysis of these results reveal a reduction in power consumption by 4.2%, 10.5%, 16.8 and 20.0% for h_2/D = 0.015, 0.04, 0.065 and 0.09, respectively, compared to the classical Scaba 6SRGT impeller. Surprisingly, this decrease is linear between h_2/D = 0 and 0.065, with a slope -22.8 (R^2=0.9993), but then deviates from linearity.

As a conclusion, it appears that if the objective is to maintain similar mixing properties, cut height must remain small (h_2/D < 0.04) and the power saving in comparison to is limited to the Scaba 6SRGT impeller is limited to about 10%.

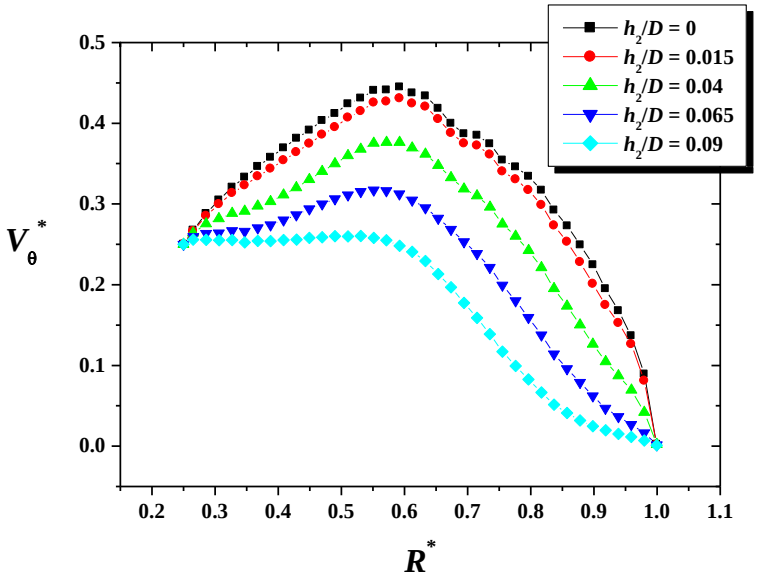

Figure 3. Normalized tangential velocity due to the impeller blade for Z^* = 0.45, Re_y = 100, l/D = 0.12, n_b = 1 as a function of R^* and h_2/D

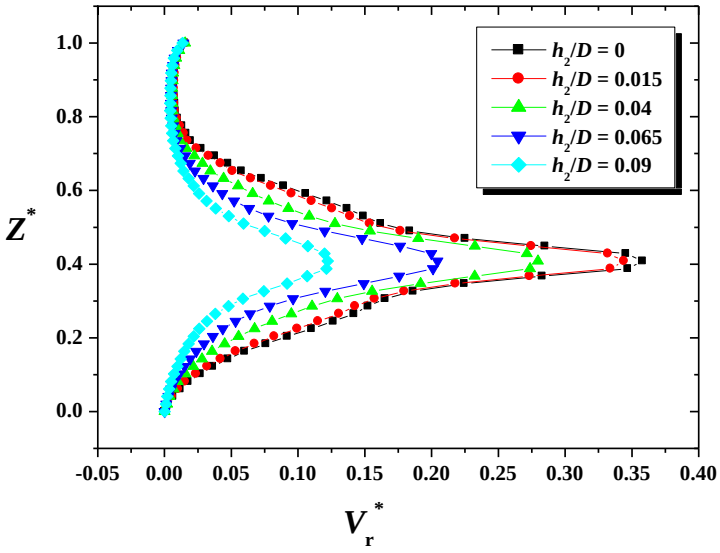

Figure 4. Normalized radial velocity profile in the impinging jet of the blade for R^* = 0.3, Re_y = 100, l/D = 0.12, n_b = 1 as a function of Z^* and h_2/D

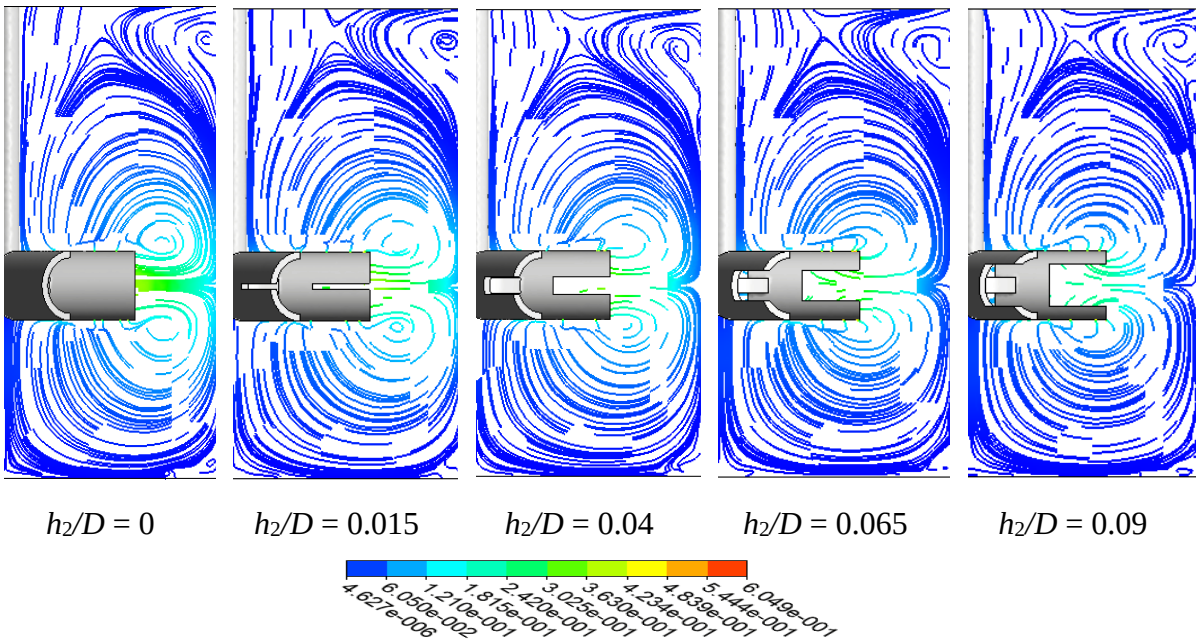

h_2/D = 0 h_2/D = 0.015 h_2/D = 0.04 h_2/D = 0.065 h_2/D = 0.09

Figure 5. Streamlines (colors based on normalized velocity) in the vertical plane of the blade for l/D = 0.12, n_b = 1, Re_y = 100 as a function of h_2/D

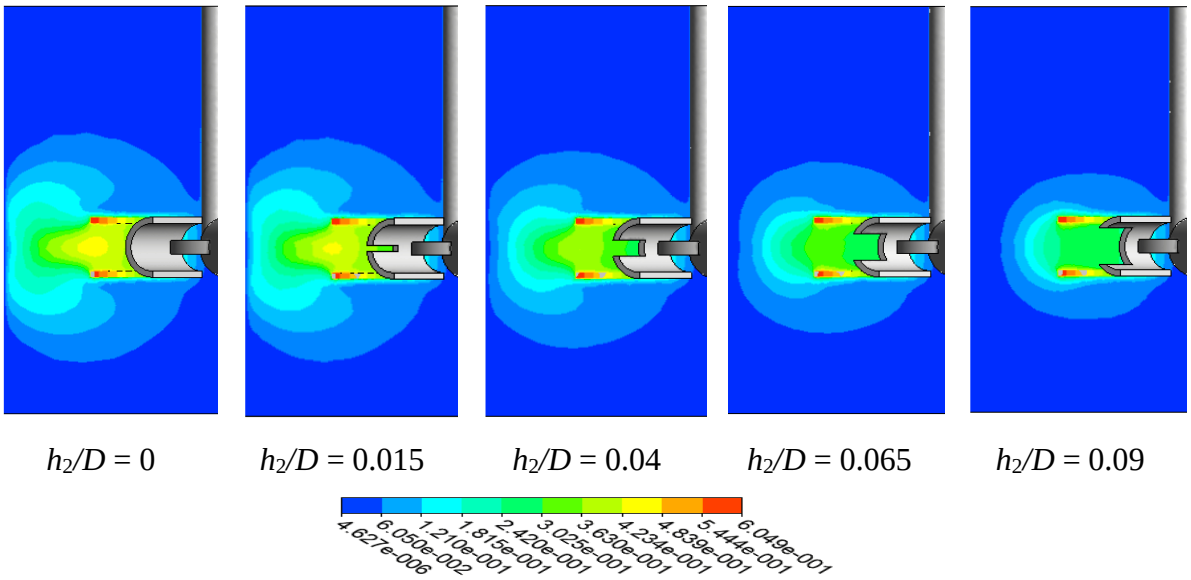

Figure 6. Normalized velocity magnitude: illustration of cavern size in the vertical plane of the blade for l/D = 0.12, n_b = 1, Re_y = 100 as a function of h_2/D

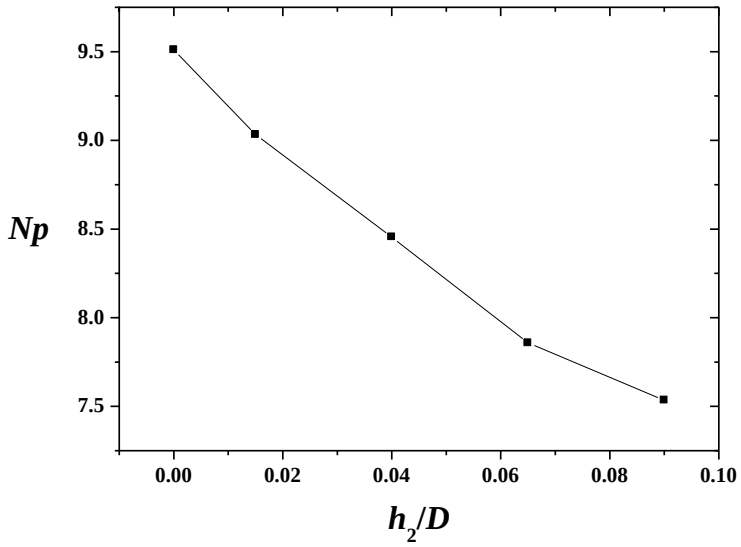

Figure 7. Power number for l/D = 0.12, n_b = 1, Re_y = 10 as a function of h_2/D

6.2. Effect of the length of cut (l)

In the second part of this section, the influence of the cut length (l) is studied. The different cases investigated are: l/D = 0 (i.e. a blade without cut), 0.06, 0.12 and 0.18, respectively. The evolution of the velocity magnitude along the vessel height (Z^*) is plotted at the radial position R^* = 0.6 for the four cases (Fig. 8). Similarly, the tangential component of velocity is monitored

along the vessel radius at the vertical position Z^* = 0.41 and plotted in Fig. 9. From the results depicted in both figures, it seems that the increased length of cut participates in the reduction of flow intensity. For example, values of $V^*_{\theta max}$ for l/D = 0, 0.06, 0.12 and 0.18 are 0.45, 0.4, 0.37 and 0.36, respectively. In both figures, it appears that the profiles mainly change when l/D<0.12: it obviously emerge that a long cut in the direction of the shaft of the impeller does not affect the flow in the tank far from the impeller anymore.

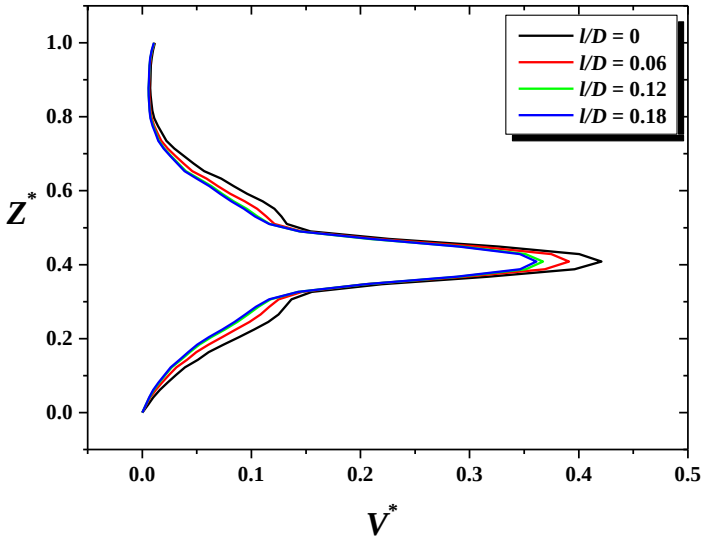

Figure 8. Dimensionless velocity at R^* = 0.6 for h_2/D = 0.04, n_b = 1, Re_y = 100 as a function of Z^* and l/D

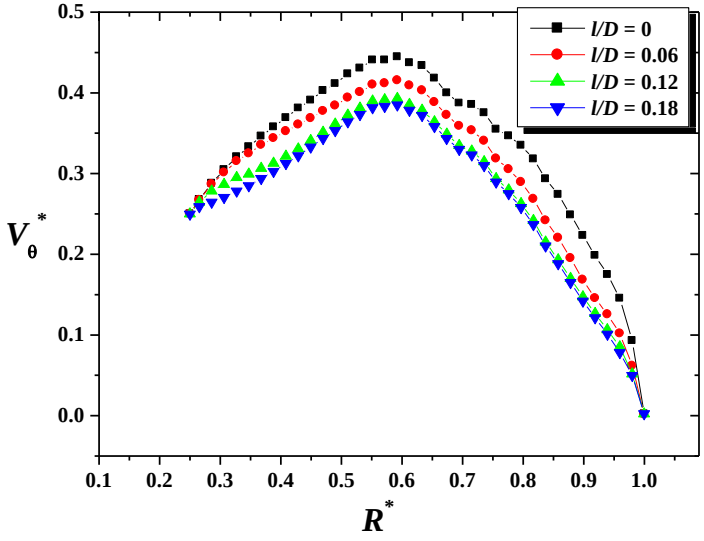

Figure 9. Dimensionless tangential velocity at $Z^* = 0.41$ for $h_2/D = 0.04$, $n_b = 1$, $Re_y = 100$ as a function of R^* and l/D

To capture further details on the effect of cut length on the hydrodynamics, the 2D streamlines are plotted for the four cases in Fig. 10. It is clearly illustrated that the cuts do not strongly alter the flow pattern, characterized by two recirculation loops, but that the axial circulation of the fluid and the radial jet impinging the wall are both weakened when the length of the cut is increased in comparison to the conventional impeller. As a consequence, the size of the recirculation loops which are formed above and below impeller is decreased with the raise of *l/D*. Near the free surface of liquid, a vortex is formed due to the absence of baffles. This vortex is intensified and enlarged with the increase of *l/D*, which is mainly due to the reduced of axial circulation of the fluid. Another consequence is that the size of the well-stirred region just around the impeller decrease progressively with the raise of *l/D*, as depicted by Fig. 11, even though this decrease is slower when $l/D>0.12$. Conversely, the increase of *l/D* seems to promote the intensification of fluid circulation in the area between consecutive baffles, which could be helpful (Fig.12).

However, it emerges from these results that an excessive increase in cut length is not beneficial in terms of cavern size and axial circulation of fluid in the whole vessel volume, but they could contribute to decrease power requirements. Thus, the results of power consumption displayed in Fig. 13 reveal an interesting decrease in N_P when cut length is increased. The values of N_P for $l/D = 0$, 0.06, 0.12 and 0.18 are 2.68, 2.37, 2.24 and 2.20, respectively, which corresponds to a decrease by about 11.56%, 16.4%, and 17.9%, compared to the blade without cut. Considering that N_P tends to a final value about 2.15 when *l/D*, these trends at $Re_y = 100$ can be fitted using the following equation:

$$N_P = 2.15 + 0.53 \cdot exp(-13.8 \cdot l/D) \quad (16)$$

As a conclusion, the effect of cut length on power saving is more limited than the effect of cut height and the effective range is limited to $l/D < 0.12$.

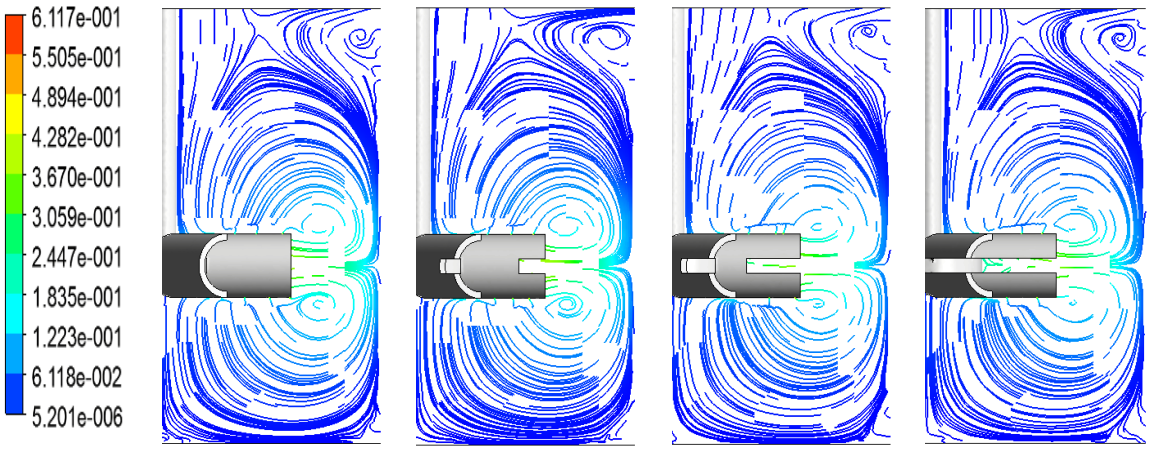

l/D = 0 l/D = 0.06 l/D = 0.12 l/D = 0.18

Figure 10. Streamlines (colors based on normalized velocity) in the vertical plane of the blade for h_2/D = 0.04, n_b = 1, Re_y = 100 as a function of l/D

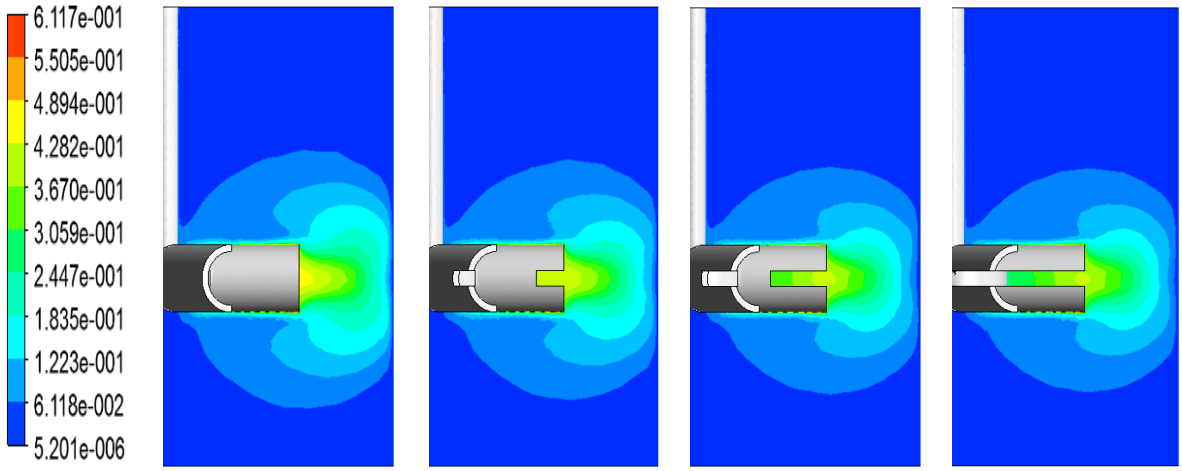

l/D = 0 l/D = 0.06 l/D = 0.12 l/D = 0.18

Figure 11. Normalized velocity magnitude: illustration of cavern size in the vertical plane of the blade for h_2/D = 0.04, n_b = 1, Re_y = 100

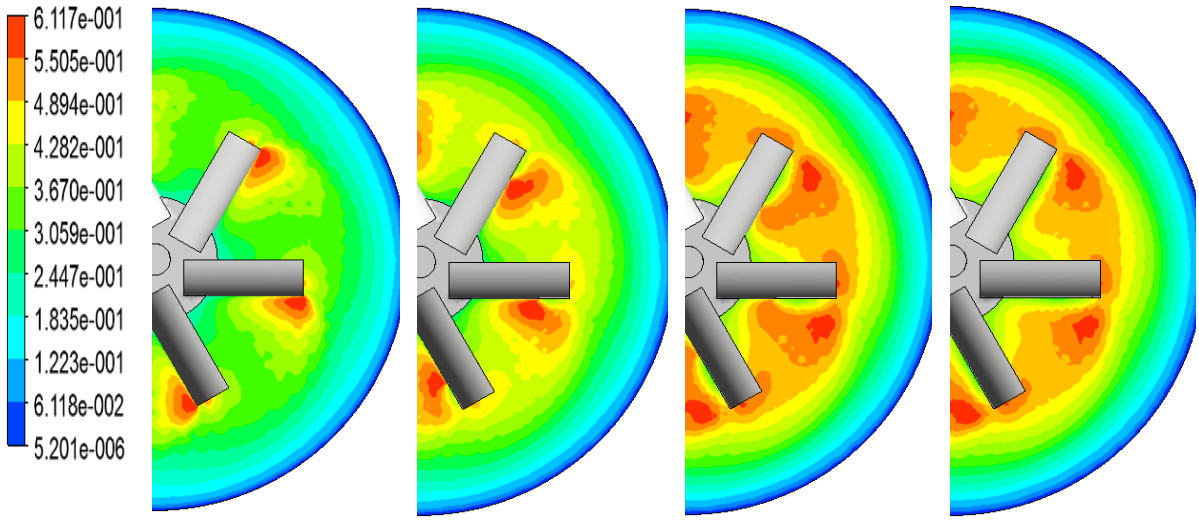

Figure 12. Normalized velocity magnitude: illustration of cavern size in horizontal plane of the blades for h_2/D = 0.04, n_b = 1, Re_y = 100 as a function of l/D

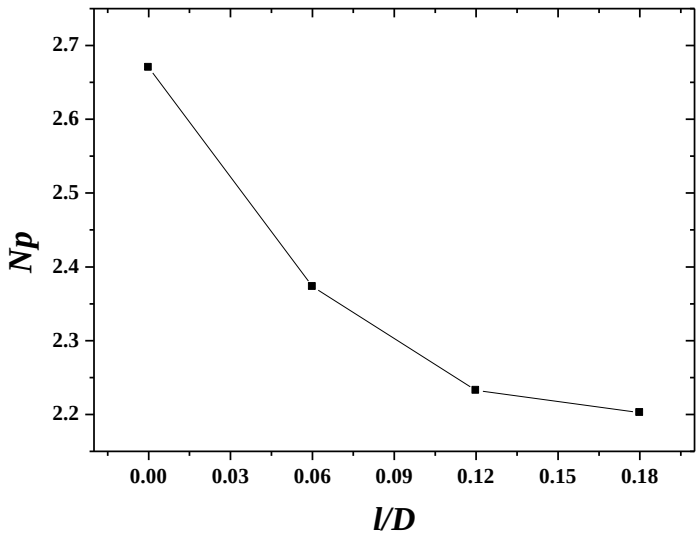

Figure 13. Power number for h_2/D = 0.04, n_b = 1, Re_y = 100 as a function of l/D

6.3. Effect of the number of cuts (n_b)

In this subsection, the effect of another geometrical parameter on the flow pattern and the power consumption due to the impeller is explored: it concerns the number of cuts (n_b). For the same cut length cut as in section 6.2 (l/D = 0.12) , five geometrical configurations were considered, which are: n_b = 1, 2, 3, 4 and 5. The tangential velocity field, the radial velocity field, and the streamlines calculated in the simulations are presented along the vessel radius,

the vessel height and in the vertical plane passing through the impeller in Fig. 14, 15 and 16, respectively. It seems that the increased number of cuts is beneficial in terms of intensification of the movement of fluid particles, the radial jet of fluid is becoming powerful and the axial circulation is highly enhanced. Consequently, the size of the well-stirred region is increased, as observed in Fig. 17. As in section 6.1, when the cut height is small, the fluid tends to follow the same velocity profile as in the conventional impeller design. So, a possible method to increase the total cut height without changing too significantly the flow pattern may consist in using several cuts. This strategy seems very efficient when n_b is increased from 1 to 2 in Fig. 14, 15 and 17, but increasing n_b appears to be useless when $n_b > 4$.

However, the price to pay to maintain the flow field close to the conventional impeller is necessarily higher power consumption or, in practice, lower power saving. Thus, power number data are depicted in Fig. 18, and the values are as follows: N_P = 1.62, 2.2, 2.34, 2.5 and 2.59 for n_b = 1, 2, 3, 4 and 5, respectively. The analysis of these results reveals an increase in N_P by about 60% from the first case n_b = 1 to the last case n_b = 5, but in comparison to the classical blade without cut (N_P = 4.86), the case n_b = 1 reveals a decrease in N_P until 66.6%. As a conclusion, even when n_b = 3, this makes it possible to approach the flow pattern of the conventional impeller with a decrease in N_P approaching 50%.

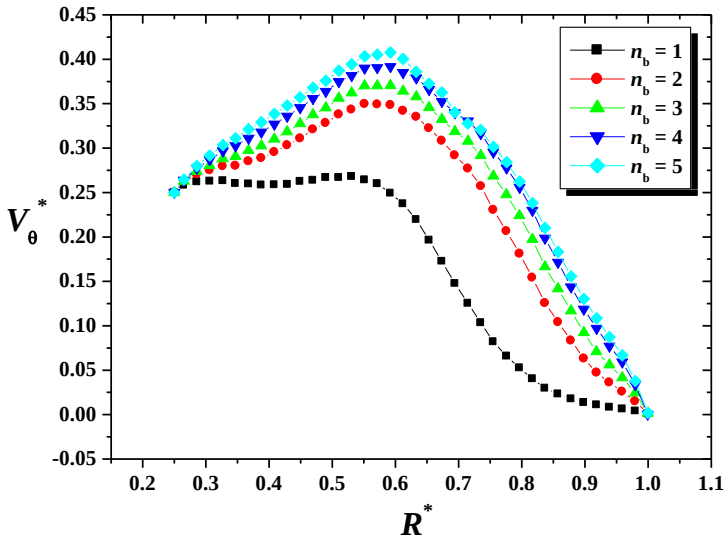

Figure 14. Normalized tangential velocity due to the impeller blade for Z^* = 0.41, Re_y = 80, l/D = 0.12 as a function of R^* and n_b

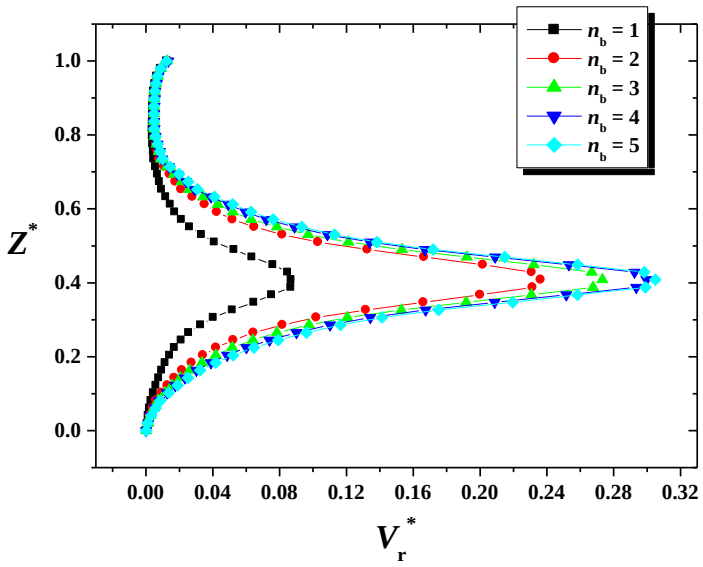

Figure 15. Normalized radial velocity profile in the impinging jet of the blade for R^* = XX, Re_y = 80, l/D = 0.12, as a function of Z^* and n_b

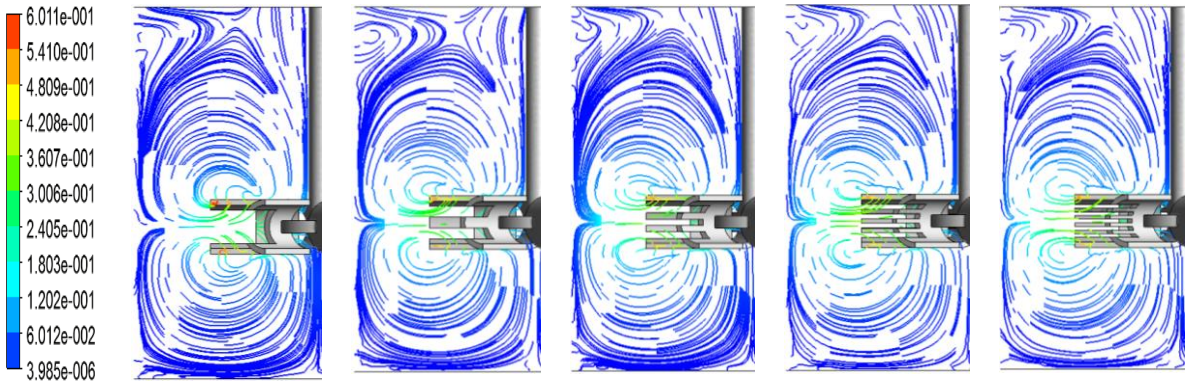

n_b = 1 n_b = 2 n_b = 3 n_b = 4 n_b = 5

Figure 16. Normalized velocity magnitude: illustration of cavern size in the vertical plane of the blade for h_2/D = 0.04, l/D = 0.12, Re_y = 80 as a function of n_b

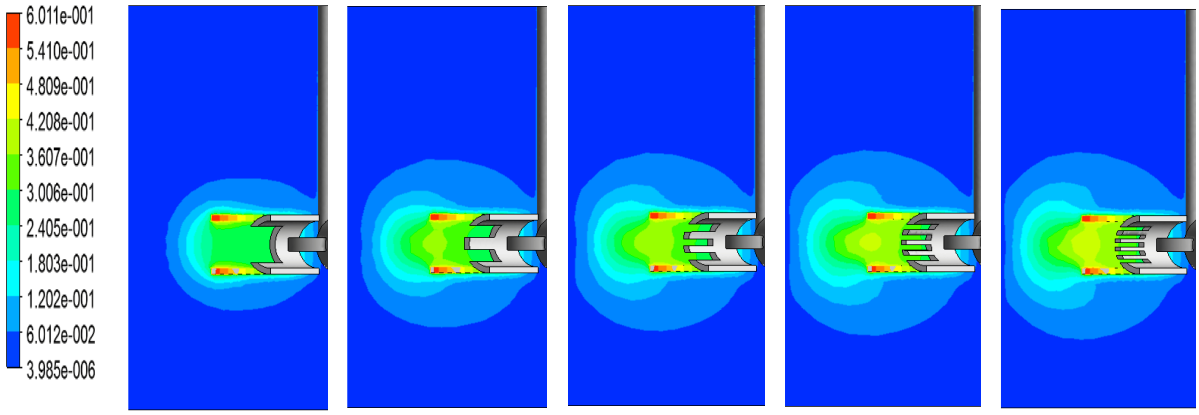

Figure 17. Normalized velocity magnitude: illustration of cavern size in the vertical plane of the blade for l/D = 0.12, Re_y = 80 as a function of n_b

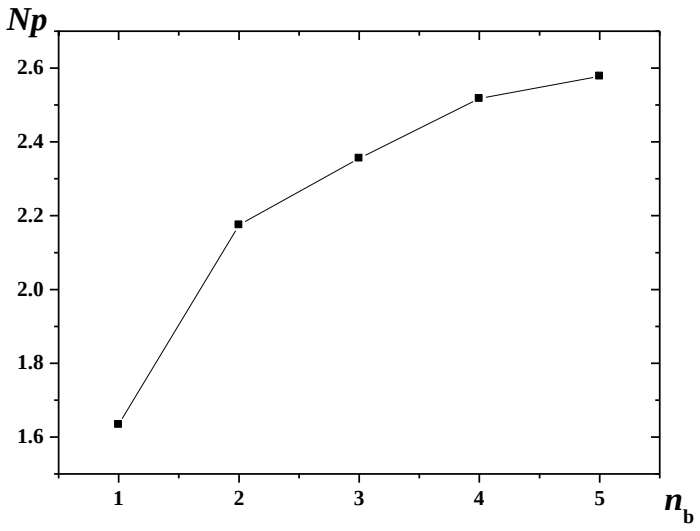

Figure 18. Power number for l/D = 0.12, Re_y = 80 as a function of n_b

7. Conclusion

Mixing of a complex non-Newtonian fluid (a shear thinning fluid with yield stress) in a cylindrical unbaffled vessel has been numerically studied. The impeller used for agitation was a six curved-blade device, the so-called Scaba 6SRGT. Cuts have been introduced in each blade in order to save power requirements. The effects of the geometry of these cuts (including the height, length and number of cuts) on the flow patterns and power consumption have been

determined. Fourteen geometrical configuration were studied to better understand the influence of these parameters both on the flow pattern and on power requirements: namely, five cases for the height of cut (h_2/D = 0, 0.015, 0.04, 0.065 and 0.09, respectively), four cases for the length of cut (l/D = 0, 0.06, 0.12 and 0.18, respectively), and five cases for the number of cuts (n_b = 1, 2, 3, 4 and 5).

The results derived from the simulations based on CFD revealed that the introduction of cuts is an interesting approach to save mechanical energy in the mixing process. However, the optimization of the cut size is not an easy task: if the increased size of cuts in blade is obviously accompanied by a reduction in power requirements, the radial impinging jet and the axial circulation of the fluid are also impaired, resulting thus in the reduction of cavern size, i.e. of the well-mixed regions. So, the overall achievements are as follows:

- The increase in cut-height from h_2/D = 0 to 0.09 yielded a reduction in power number from 4.21% to 20% compared to the classical Scaba 6SRGT impeller without cut, but it impaired strongly the flow pattern and, therefore, the mixing effectiveness.
- The increase in cut-length from for l/D = 0, 0.06, 0.12 lead to a decrease by about of power number 11.56%, 16.4%, and 17.9%, compared to the blade without cut; thus, the effect of l/D is less significant than that of height, and a further increase in l/D lead to insignificant changes.
- The increase in the number of cuts from n_b = 1 to 5 yielded a decrease by about 60% and the comparison between the case n_b = 1 and the classical blade without cut revealed a reduction in N_P until 66.6%, but to approach the mixing features of the conventional impeller, $n_b > 2$ must be preferred, whereas $n_b > 4$ leads to insignificant changes.

The analysis of these findings allows us to select the case with n_b = 3 and l/D = 0.12 as a trade-off between reduced power consumption and enlarged cavern size. In comparison to the conventional Scaba 6SRGT impeller, a reduction in power number by about 50% is achieved, whereas the features of the field are only slightly affected.

Now, it is clear that further investigations on the suggested design are needed for different kinds of fluids with various rheological properties in order to define how optimum cut geometry may change with fluid properties. For this purpose, the methodology developed in this work will be helpful.

Nomenclature

b_t – blade thickness, m

c - impeller off-bottomed clearance, m

d - blade diameter, m

D - tank diameter, m

d_s –shaft diameter, m

d_t – disc thickness, m

e – impeller eccentricity, m

h - blade height, m

H - liquid level, m

h_2 - height of cut in blade, m

l - length of cut in blade, m

K - consistency index, Pa s^n

K_s - Metzner-Otto's constant, -

n - flow behavior index, -

N - impeller rotational speed, 1/s

n_b - number of blade, -

P – power, W

N_P - power number, -

N_Q - flow number, -

Q_p - pumping flow rate, m^3/s

Q_v - viscous dissipation function, $1/s^2$

R - radial coordinate, m

R^* - dimensionless radial coordinate, -

Re_y - Reynolds number for a yield stress fluid, -

V – velocity magnitude, m/s

V_z - axial velocity, m/s

V_θ - tangential velocity, m/s

V_r - radial velocity, m/s

Z – axial coordinate, m

Z^* - dimensionless axial coordinate, -

Greek letters

γ_{avg} - average shear rate, 1/s

η - apparent viscosity, Pa.s

θ - angular coordinate, degree

ρ - fluid density, kg/m^3

τ - shear stress, Pa

τ_y - suspension yield stress, Pa

ω - angular velocity, rad/s

References

Ameur, H. 2016a. Mixing of complex fluids with flat and pitched bladed impellers: effect of blade attack angle and shear-thinning behavior. Food Bioprod. Process. 99, 71–77.

Ameur, H. 2016b. 3D hydrodynamics involving multiple eccentric impellers in unbaffled cylindrical tank. Chin. J. Chem. Eng. 24, 572–580.

Ameur, H., Bouzit, M., Ghenaim, A. 2015. Numerical study of the performance of multistage Scaba 6SRGT impellers for the agitation of yield stress fluids in cylindrical tanks. J. Hydrodyn. Ser. B 27, 436–442.

Ameur, H., Ghenaim, A. 2018. Mixing of complex fluids in a cylindrical tank by a modified anchor impeller. ChemistrySelect 3, 7472–7477.

Bao, Y., Bo, Y., Gao, Z., Zhang, Z., Liu, T., Gao, X., 2011. Power demand and mixing performance of coaxial mixers in non-Newtonian fluids. J. Chem. Eng. Japan 44, 57–66.

Beloudane, M, Bouzit, M, Ameur, H. 2018. Numerical investigation of the turbulent flow generated with a radial turbine using a converging hollow blade. Polish J. Chem. Technol. 20, 129–137.

Cortada-Garcia, M., Dore, V., Mazzei, L., Angeli, P. 2017. Experimental and CFD studies of power consumption in the agitation of highly viscous shear thinning fluids. Chem. Eng. Res. Des. 119, 171–182.

Devi, T.T., Kumar, B., 2013. Comparison of flow patterns of dual Rushton and CD-6 impellers. Theor. Found. Chem. Eng. 47, 344–355.

Foukrach, M., Bouzit, M., Ameur, H., Kamla, Y. 2016. Influence of the vessel shape on the performance of a mechanically agitated system. Chem. Pap. 73, 469–480.

Ghotli, R.A., Abdul Aziz, A.R., Ibrahim, S. 2016. The effect of various designs of six-curved blade impellers on reaction rate analysis in liquid liquid mixing vessel. Measurement 91, 440–450.

Ghotli, R.A., Abdul Aziz, A.R., Ibrahim, S., Baroutian, S., Arami-Niya, A. 2013. Study of various curved-blade impeller geometries on power consumption in stirred vessel using response surface methodology. J. Taiwan Inst. Chem. Eng. 44, 192–201.

Kazemzadeh, A., Ein-Mozaffari, F., Lohi, A., Pakzad, L. 2016a. Investigation of hydrodynamic performances of coaxial mixers in agitation of yield-pseudoplasitc fluids: Single and double central impellers in combination with the anchor. Chem. Eng. J. 294, 417–430.

Kazemzadeh, A., Ein-Mozaffari, F., Lohi, A., Pakzad, L. 2016b. A new perspective in the evaluation of the mixing of biopolymer solutions with different coaxial mixers comprising of two dispersing impellers and a wall scraping anchor. Chem. Eng. Res. Des. 114, 202–219.

Kazemzadeh, A., Ein-Mozaffari, F., Lohi, A., Pakzad, L. 2017. Intensification of mixing of shear-thinning fluids possessing yield stress with the coaxial mixers composed of two different central impellers and an anchor. Chem. Eng. Process. Process Intensif. 111, 101–114.

Macosko, C.W. 1994. Rheology: Principles, Measurements & Applications. Wiley-VCH, New York, 47–49.

Malik, D., Pakzad, L. 2018. Experimental investigation on an aerated mixing vessel through electrical resistance tomography (ERT) and response surface methodology (RSM). Chem. Eng. Res. Des. 129, 327–343.

Metzner, B., Otto, R.E. 1957. Agitation of non-Newtonian fluids. AIChE J., 3, 3–11.

Pakzad, L., Ein-Mozaffari, F., Chan, P. 2008a. Using computational fluid dynamics modeling to study the mixing of pseudoplastic fluids with a Scaba 6SRGT impeller. Chem. Eng. Process. Process Intensif. 47, 2218–2227.

Pakzad, L., Ein-Mozaffari, F., Chan, P. 2008b. Using electrical resistance tomography and computational fluid dynamics modeling to study the formation of cavern in the mixing of pseudoplastic fluids possessing yield stress. Chem. Eng. Sci. 63, 2508–2522.

Pakzad, L., Ein-Mozaffari, F., Upreti, S. R., Lohi, A. 2013a. Agitation of Herschel–Bulkley fluids with the Scaba–anchor coaxial mixers. Chem. Eng. Res. Des. 91, 761–777.

Pakzad, L., Ein-Mozaffari, F., Upreti, S. R., Lohi, A. 2013b. A novel and energy-efficient coaxial mixer for agitation of non-Newtonian fluids possessing yield stress. Chem. Eng. Sci. 101, 642–654.

Pakzad, L., Ein-Mozaffari, F., Upreti, S. R., Lohi, A. 2013c. Using tomography to assess the efficiency of the coaxial mixers in agitation of yield-pseudoplastic fluids. Chem. Eng. Res. Des. 91, 1715–1724.

Rudolph, L., Atiemo-Obeng, V., Schaefer, M., Kraume, M., 2009. Power consumption and blend time of coaxial tank mixing systems in non-Newtonian fluids. In: Proceedings of the 13th European Conference Mixing, London, United Kingdom, pp. 439–446.

Saeed, S., Ein-Mozaffari, F., Upreti, S.R., 2007. Using computational fluid dynamics and ultrasonic Doppler velocimetry to study pulp suspension mixing. Ind. Eng. Chem. Res. 46, 2172–2179.

Yao, W. G., Sato, H., Takahashi, K., Koyama, K. 1998. Mixing performance experiments in impeller stirred tanks subjected to unsteady rotational speeds. Chem. Eng. Sci. 53, 3031–3040.

Zhao, J., Gao, Z., Bao, Y. 2011. Effects of the blade shape on the trailing vortices in liquid flow generated by disc turbines. Chin. J. Chem. Eng. 19, 232–242.

Zheng, Z., Sun, D., Li, J., Zhan, X., Gao, M. 2018. Improving oxygen transfer efficiency by developing a novel energy-saving impeller. Chem. Eng. Res. Des. 130, 199–207.

Zheng, Z., Sun, D., Zhan, X., Gao, M., 2017. Gas–liquid dispersion impeller assembly with annular-sector-shaped concave blades. US Patent Application no. 15, 548, 080.